HETEROCYCLES, Vol. 106, No. 1, 2023, pp. 67 - 81. © 2023 The Japan Institute of Heterocyclic Chemistry
Received, 9th September, 2022, Accepted, 31st October, 2022, Published online, 8th November, 2022
DOI: 10.3987/COM-22-14745

DESIGN, SYNTHESIS AND BIOLOGICAL EVALUATION OF PYRIMIDINAMINE DERIVATIVES CONTAINING UREA MOIETY

Weiqin Liu,[1#] Mi Hou,[1#] Qin Wang,[1] Huayuan Tan,[1] Litao Ji,[1] Congyu Wang,[1] Xuesha Long,[1] Zhenchao Wang,[1,2,3]* and Guiping Ouyang[1,2,3]*

[1] School of Pharmaceutical Sciences, Guizhou University, Guizhou Guiyang, 550025, China; [2] Key Laboratory of Green Pesticide and Agricultural Bioengineering, Ministry of Education, Guiyang, 550025, China; [3] Guizhou Engineering Laboratory for Synthetic Drugs, Guiyang, 550025, China. [#] These authors contributed equally to this work. Email: wzc.4884@163.com, gpouyang@gzu.edu.cn

Abstract – New series of 17 pyrimidinamine derivatives containing urea moiety were designed and synthesized. Their antitumor activity was investigated by MTT method. The results showed that some of these compounds exhibited moderate to good antitumor activities against all four cancer cell lines. The IC_{50} value of compound **HD-6** on PC-3 cells was better 2.37 μM than the positive control drug sorafenib (3.66 μM). The inhibitory activity of most target compounds on HepG2 cells was better than that of positive drug sorafenib (10.70 μM). Among them, the IC_{50} value of compound **HD-6** on K562 cells was 6.80 μM, which close to solafinib (4.62 μM). Further studies revealed that compound **HD-6** clearly possessed apoptosis inducing effects, increased the level of reactive oxygen species, arrested the cycle in the G2/M phase and regulated the expression of tyrosine kinase EGFR in PC-3 cells.

INTRODUCTION

It has been reported that pyrimidine and its fused pyrimidine derivatives are a class of heterocyclic scaffolds that possess a range of biological and pharmacological activities,[1] for example, anticancer,[2] antimicrobial,[3] antioxidant,[4] antidepressant,[5] antiviral,[6] and anxiolytic activities.[7] Because of the extensive pharmacological and biological activities of pyrimidine,[8] the action targets of pyrimidine were conducted in-depth studies. Many studies show the targets of pyrimidine derivatives are beneficial to cancer treatment.[9-11]

Pyrimidinamine is widely distributed in organisms and has a wide range of biological activities.[12] Such as antitumor properties,[13] herbicides,[14] antibacterial,[15] antidepressant,[16] antiviral.[17] It has been reported that pyrimidinamine derivatives can be used as B-cell lymphoma 6 inhibitors to treat diffuse large B-cell lymphoma.[18] Moreover, pyrimidinamine derivatives also act as ER antagonists and VEGFR-2 inhibitors in the treatment of estrogen receptor-positive breast cancer.[19] Zimmermann et al. synthesized a series of pyrimidinamine derivatives, which can be used as protein kinase C (PKC) inhibitors. PKC inhibitors are useful for the synthesis and clinical use of various effective drugs to treat tumors, cardiovascular diseases, hypertension, etc.[20] Based on the above research findings, pyrimidinamine derivatives have attracted more and more attention due to their important roles in pharmaceutical and biological processes.

The urea NH moiety is a favorable hydrogen bond donor, while the urea oxygen atom is considered an excellent acceptor. Following the successful development of sorafenib, many new compounds containing urea moiety have been synthesized and evaluated for their antitumor activity.[21]

In this study, we used different substituted aniline as raw materials to obtain pyrimidinamine derivatives containing urea **HD-1**-**HD-17**. All the unreported compounds were characterized and confirmed by ^{1}H, ^{13}C NMR and HRMS. The anti-tumor activity of these compounds were evaluated by the methyl thiazolyl tetrazolium (MTT) assay. The results showed that these compounds against A549, PC-3, HepG2 and K562 cell lines with good activity. Further mechanism studies revealed that compound **HD-6** promoted the apoptosis of PC-3 cells. At the same time, compound **HD-6** could enhance reactive oxygen level and arrest cell cycle in G2/M phase in PC-3 cells. Western blotting assay further demonstrated that compound **HD-6** could regulate the expression of tyrosine kinase EGFR.

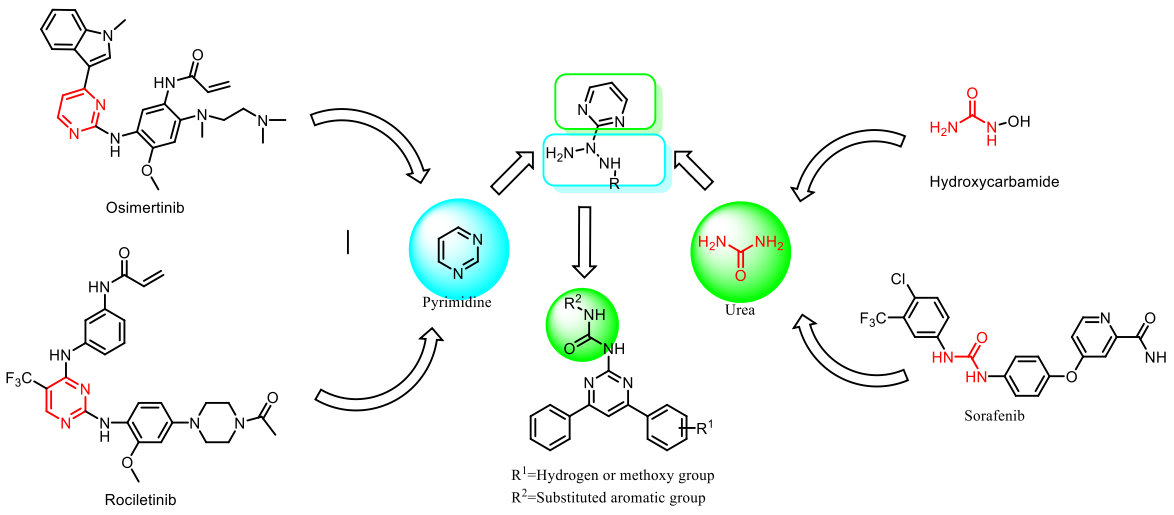

Figure 1. Design strategy of the target compounds

RESULTS AND DISCUSSION

Chemistry

The preparation of target compounds was shown in **Scheme 1**, the intermediate 4-acetylphenyl isocyanate **2** was prepared by condensation of anilines with triphosgene in the presence of triethylamine in CH_2Cl_2. Chalcone **4** can be achieved from substituted benzaldehyde reacted with acetophenone under alkaline condition, the key intermediate 4,6-diarylpyrimidinyl-2-amine **5** was obtained after *trans*-chalcone **4** reacted with guanidine hydrochloride. Finally, the key intermediate **5** reacted with intermediate **2** to obtain the target compounds **HD-1**-**HD-17**. All the unreported compounds were characterized and confirmed by ^1H, ^{13}C NMR and HRMS spectral studies (Supporting Information).

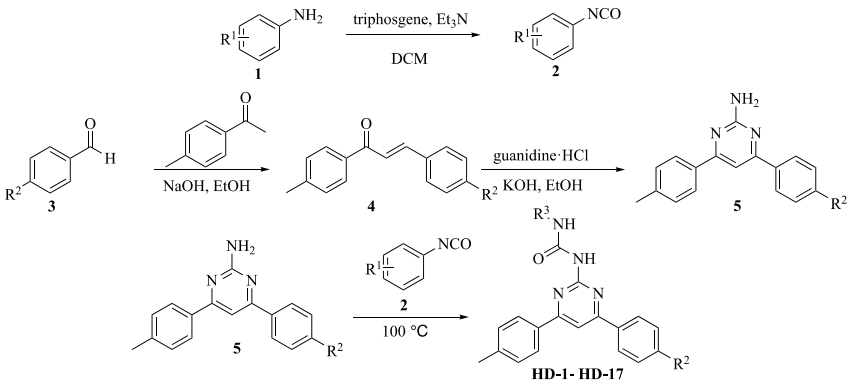

HD-1 R^2=H, R^3=4-Me-phenyl
HD-2 R^2=H, R^3=3-Me-phenyl
HD-3 R^2=H, R^3=2-Cl-phenyl
HD-4 R^2=H, R^3=3-Cl-phenyl
HD-5 R^2=H, R^3=Bn-phenyl
HD-6 R^2=H, R^3= naphthyl
HD-7 R^2=H, R^3=4-Cl-phenyl
HD-8 R^2=H, R^3=4-F-phenyl
HD-9 R^2=4-OMe, R^3=3-Me-phenyl
HD-10 R^2=4-OMe, R^3=4-Me-phenyl
HD-11 R^2=4-OMe, R^3=2-Cl-phenyl
HD-12 R^2=4-OMe, R^3=3-Cl-phenyl
HD-13 R^2=4-OMe, R^3=4-Cl-phenyl
HD-14 R^2=4-OMe, R^3=3-F-phenyl
HD-15 R^2=4-OMe, R^3=3-CF_3-phenyl
HD-16 R^2=4-OMe, R^3=Bn-phenyl
HD-17 R^2=4-OMe, R^3= naphthyl

Scheme 1. Synthetic route of the target compounds

Biological activity

Evaluation of cytotoxicity

The antitumor potency of the pyrimidinamine derivatives containing urea compounds were evaluated on human NSCLC cell line A549, human prostate cancer cell line PC-3, human chronic myeloid leukemia cell line K562 and human hepatoma cell line HepG2 by the MTT assay, with sorafenib as positive control drug. The inhibition rates of 17 compounds on four tumor cell lines at 10 μM are shown in **Table 1**. The results showed that the target compound **HD-1**-**HD-17** had moderate to good activities on PC-3 and HepG2 cell lines after acting for 48 h, while the effect on A549 and K562 was relatively weak. The average IC_{50} value of compound **HD-11**, **HD-14**, and **HD-15** on A549 cells was 16.55 μM, 16.57 μM and 17.99 μM. Among PC-3 cells, the IC_{50} value of compound **HD-4**, **HD-7**, **HD-9**, **HD-14** was 7.54 μM, 4.98 μM, 5.66 μM, and 4.84 μM, especially, compound **HD-6** possessed the best activity against PC-3

cells and the IC_{50} value was as low as 2.37 μM. Most of the compounds had good activity against HepG2 cells, and their IC_{50} values were better than the positive control drug sorafenib (IC_{50}=10.70 μM). The IC_{50} value of compound **HD-15** on K562 cells was 6.8 μM and compound **HD-17** was 8.29 μM (**Table 2**). According to the preliminary analysis of the structure-activity relationship, it was found that when the substituents on the benzene ring were halogen and electron-withdrawing groups, the activities of the compounds against PC-3 and HepG2 cells were increased. For HepG2 cells, the *p*-trifluoromethyl group could improve the inhibitory activity and the activity of *o*-chlorine substitution on benzene ring is better than that of *p*-chlorine substitution. But for PC-3 cells, the activity of *p*-chlorine substitution is better than that of *o*-chlorine substitution and *m*-chlorine substitution.

Table 1. The inhibition rate against cancer cell lines of target compounds **HD-1**-**HD-17** at 10 μM

Comp.	Inhibition rate[a]±SD (Concentration: 10 μM)			
	A549	PC-3	HepG2	K562
HD-1[b]	6.55±4.27	5.60±8.88	23.84±4.49	15.64±5.14
HD-2[b]	17.96±2.52	24.02±4.88	49.13±1.27	28.54±1.15
HD-3[b]	9.79±4.91	32.06±3.16	32.06±3.16	18.08±0.45
HD-4[b]	15.42±2.65	32.45±2.55	32.45±2.55	16.05±5.28
HD-5[b]	6.69±0.81	27.70±3.17	27.70±3.17	25.53±0.97
HD-6[b]	11.24±1.25	62.31±7.46	62.31±7.46	43.23±2.41
HD-7[b]	24.69±4.41	53.72±1.01	53.35±0.72	19.47±6.27
HD-8[b]	10.80±1.17	35.79±0.67	33.88±2.72	18.17±4.51
HD-9[b]	10.42±1.15	30.32±4.38	33.30±1.96	16.67±1.81
HD-10[b]	10.58±2.74	11.79±3.77	36.20±3.53	15.91±1.28
HD-11[b]	31.31±4.07	17.53±2.28	52.87±6.28	2.81±1.07
HD-12[b]	26.13±1.65	26.53±4.41	56.08±3.62	28.48±4.57
HD-13[b]	22.80±4.52	14.78±5.65	33.21±0.71	37.99±7.12
HD-14[b]	25.03±1.64	32.31±9.42	36.92±3.40	20.18±3.81
HD-15[b]	27.71±2.57	22.92±4.41	52.17±3.90	53.42±1.64
HD-16[b]	18.09±2.21	27.55±1.87	32.75±7.81	36.99±5.06
HD-17[b]	18.48±2.39	24.83±0.70	32.83±8.24	45.37±6.44
Sorafenib[c]	51.49±1.65	61.61±1.07	66.60±3.70	79.05±0.86

[a] Average of the three trials. [b] Compound that could not dissolve in the assay system. [c] Commercial sorafenib was used as positive control.

Table 2. IC_{50} values for A549, PC-3, HepG2, K562 cell lines

Comp.	IC_{50}[a]±SD/(μM)			
	A549	PC-3	HepG2	K562
HD-1[b]	>50	>50	26.55±9.86	22.96±5.10
HD-2[b]	32.37±3.33	31.83±3.51	7.55±0.54	16.68±3.42
HD-3[b]	>50	10.25±3.30	16.94±2.90	31.48±5.76
HD-4[b]	42.36±4.90	7.54±0.62	37.13±5.97	29.94±7.07
HD-5[b]	>50	16.80±2.02	19.69±4.69	17.15±3.05
HD-6[b]	>50	2.37±0.49	10.40±1.86	9.93±2.18
HD-7[b]	30.33±1.89	4.98±0.84	9.99±5.12	31.50±6.34
HD-8[b]	>50	11.70±0.45	19.37±4.03	26.31±0.49
HD-9[b]	>50	5.66±0.65	18.69±2.98	17.71±4.65
HD-10[b]	>50	27.71±3.75	12.36±0.94	27.80±3.56
HD-11[b]	16.55±4.11	37.68±5.16	9.89±3.34	>50
HD-12[b]	23.91±0.93	22.26±2.11	9.55±1.53	19.64±0.89
HD-13[b]	22.09±3.27	25.19±1.89	14.58±0.98	13.95±0.65
HD-14[b]	16.57±2.30	4.84±0.64	9.79±1.65	27.12±3.07
HD-15[b]	17.99±1.88	17.61±2.44	5.43±0.90	6.80±3.49
HD-16[b]	23.05±4.83	16.44±0.19	25.80±8.70	10.73±0.44
HD-17[b]	35.93±4.73	24.57±3.28	35.55±6.10	8.29±0.30
Sorafenib[c]	6.03±0.75	3.66±0.48	10.70±0.50	4.62±0.31

[a] Average of the three trials. [b] Compound that could not dissolve in the assay system. [c] Commercial Sorafenib was used as positive control.

Apoptosis of compound HD-6

In order to further explore the antitumor mechanism of compound **HD-6** on PC-3 cell line, the effect of compound **HD-6** on apoptosis of PC-3 cells was tested with sorafenib as a positive control. As shown in **Figure 2**, after co-culturing compound **HD-6** (0, 8, 12, 16, 20 μM) and PC-3 cells for 48 h, DAPI staining experiment showed that compound **HD-6** caused shrinkage and nuclear chromatin condensation in PC-3 cells, suggesting apoptosis, and the number of apoptotic cells is concentration-dependent. And the cell apoptosis of PC-3 cells induced by different concentrations of compound **HD-6** (0, 8, 12, 16, 20 μM) for 48 h was evaluated using Annexin V-FITC/PI double-staining technique, and the apoptosis ratio of PC-3 cells was detected by flow cytometry. According to the results, it can be clearly seen that the ratio of apoptotic (early and late) cells induced by compound **HD-6** obviously increased in a dose-dependent manner compared to control group. When the concentration of compound **HD-6** was 0, 8, 12, 16 and 20 μM, the apoptosis rates are as follows: 4.07%, 28.26%, 47.80%, 64.06%, and 66.55%. The results showed that compound **HD-6** could induce apoptosis in PC-3 cells.

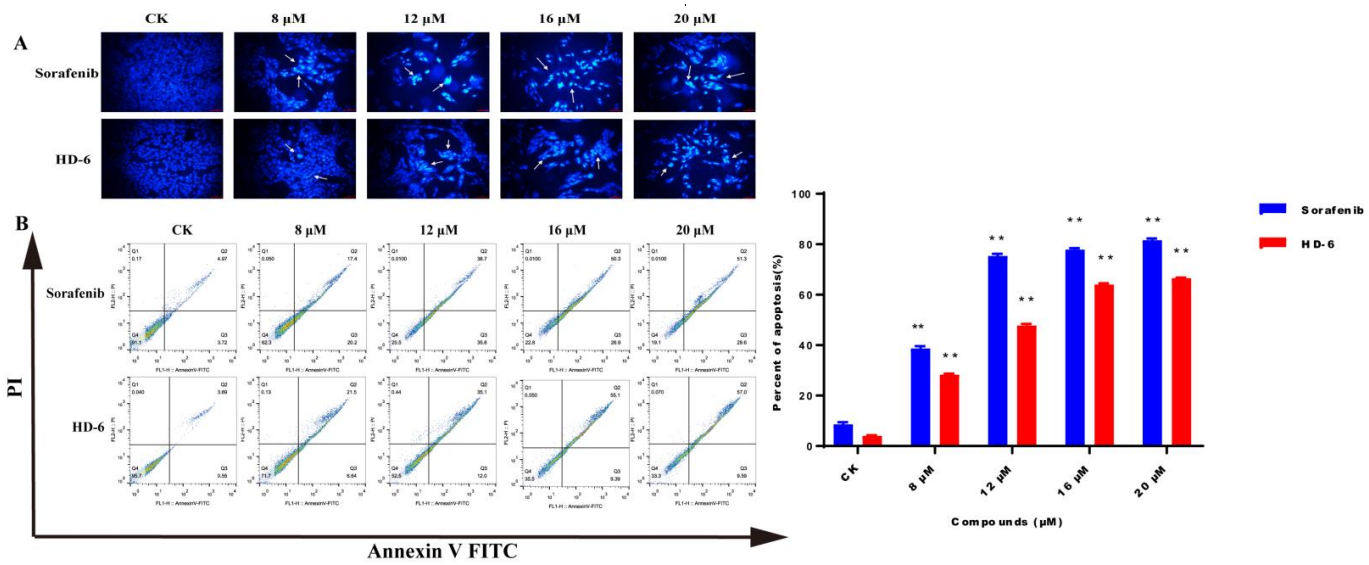

Figure 2. Apoptosis of compound **HD-6**

A. DAPI staining results of compound **HD-6** and sorafenib. B. Apoptosis graphs and statistical graphs of compound **HD-6** and sorafenib. ** $p<0.01$.

Reactive oxygen species of compound HD-6

The elevated level of reactive oxygen species (ROS) is a sign of cancer.[22] Although the increased ROS concentration plays an important role in the formation and progress of cancer, the level higher than the threshold of cytotoxicity will lead to the death of cancer cells.[23] As some widely used anticancer therapies (such as radiotherapy and chemotherapy) rely on ROS accumulation as a mechanism to induce cancer cell death[24], the ability of cancer cells to control ROS levels is the driving factor of drug resistance and a key consideration for successful cancer treatment.[25] After compound **HD-6** and sorafenib were co-cultured with PC-3 cells at the same concentration as the apoptosis experiment for 24 hours. We used fluorescent probe DCFH-DA to detect the changes of reactive oxygen species (ROS) in PC-3 cells. As shown in **Figure 3**, the results of flow cytometry showed that compound **HD-6** and positive control drug sorafenib, could significantly increase the ROS level in PC-3 cells.

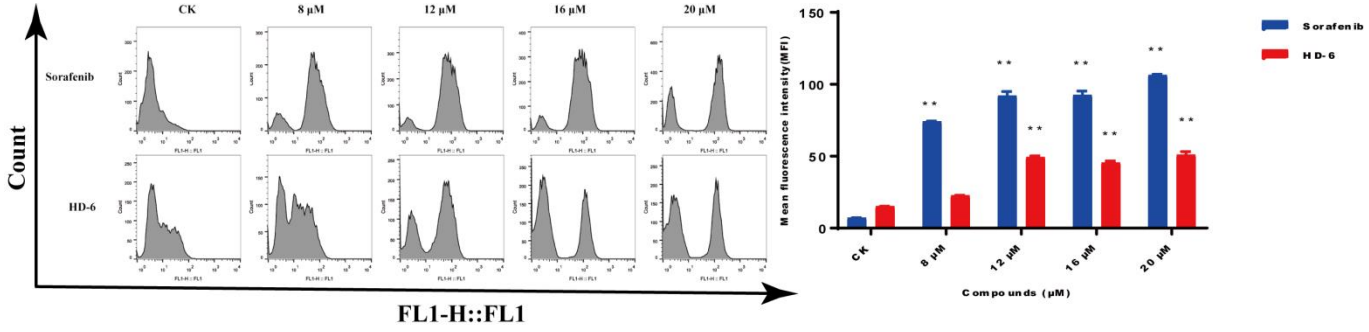

Figure 3. Level of reactive oxygen species of compound **HD-6**. ** $p<0.01$.

Analysis of cell cycle of compound HD-6

One of the main characteristics of cancer cells is the disorder of cell cycle control. Maintaining the stability of cell cycle is the key to cancer treatment.[26] After PC-3 cells were treated with different concentrations of compound **HD-6** (0, 8, 12, 16, 20 μM) for 24 h. The intracellular DNA was stained with PI staining and the changes of cell cycle were detected by flow cytometry. As shown in **Figure 4**, the results of this study showed that compound **HD-6** induced cell cycle arrest at G2/M phase and so inhibited the proliferation of PC-3 cells. When the concentration of compound **HD-6** was 0, 8, 12, 16 and 20 μM, the rates of PC-3 cells in G2/M phase are as follows: 27.57%, 30.23%, 36.63%, 37.00%, and 38.43%. The results showed that the proportion of G2/M phase cells arrested by compound **HD-6** increased in a concentration-dependent manner.

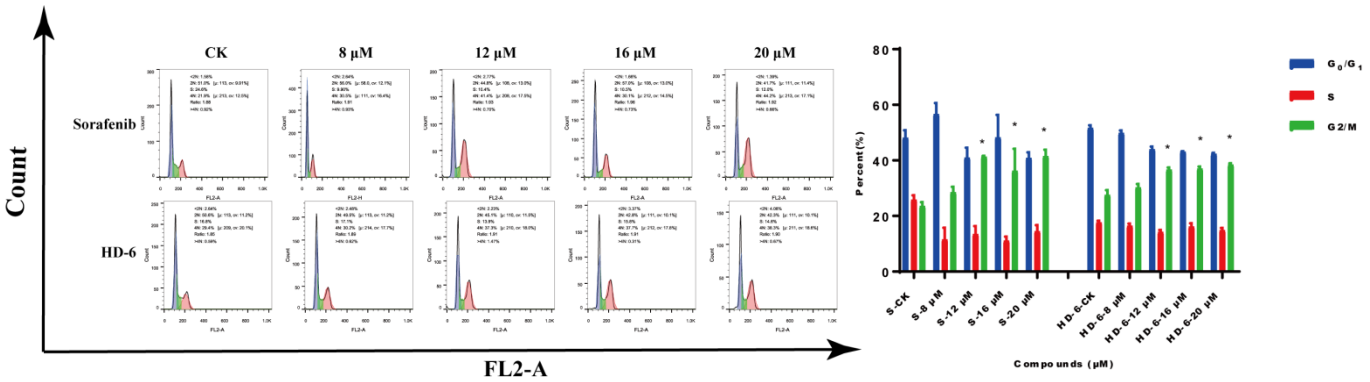

Figure 4. The results of the cycle experiment. * $p<0.05$.

Western blotting experiment of HD-6

Finally, the functions of compound **HD-6** in the expression of EGFR and active EGFR was estimated through western blotting assay. In **Figure 5**, EGFR and phosphorylated EGFR (Tyr1068) protein levels

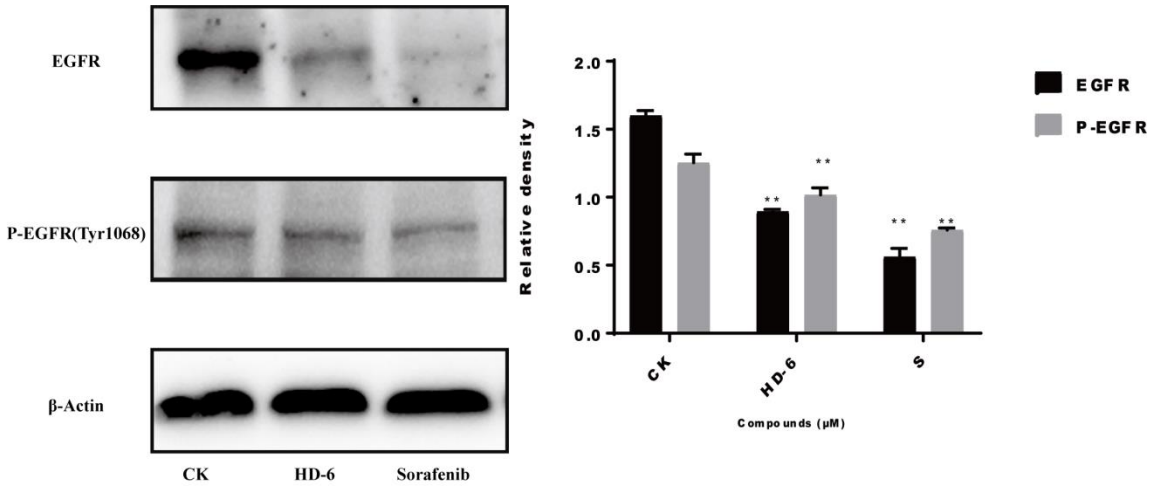

Figure 5. Detection of EGFR expression in PC-3 by western blotting. ** $p<0.01$.

were hindered by compound **HD-6** management at the concentrations of 12 μM. The results showed that compound **HD-6** and sorafenib can inhibited cell growth by suppressing the activity of EGFR, especially the expression of p-EGFR (Tyr1068).

CONCLUSIONS

In our study, new series of 17 pyrimidinamine derivatives containing urea moiety were designed and synthesized. Most of these compounds had good inhibitory activities against the tested cells (A549, PC-3, HepG2 and K562). Compound **HD-6** was selected for further investigation including for its mechanism of growth inhibition on the PC-3 cell line. The results of DAPI reagent staining showed that PC-3 cells had the phenomenon of cell shrinkage and nuclear chromatin condensation after treated with compound **HD-6.** Flow cytometry result further proved compound **HD-6** could induce the apoptosis of PC-3 cells. The level of reactive oxygen species in PC-3 cells was detected by flow cytometry, the results suggested that compound **HD-6** could increase the level of ROS in PC-3 cells. The results of cell cycle experiment demonstrated that compound **HD-6** can arrest PC-3 cells in G2/M phase. In summary, these results lay a foundation for further structural optimization of pyrimidinamine derivatives containing urea moiety as anti-tumor compounds.

EXPERIMENTAL

Materials

Unless otherwise stated, all chemicals and solvents are chemically pure or analytically pure. The melting point of the compound was measured on X-4 binocular microscope (Beijing Tech Instrument Co., China) without correction. The nuclear magnetic resonance spectrum was recorded by JEOL- ECX500 nuclear magnetic resonance instrument. The nuclear magnetic resonance instrument works at 500 and 126 MHz frequencies at room temperature, spectrometer with DMSO-d_6 as solvent and TMS as internal standard. The methanol solubility and HRMS-ESI spectra of the target compounds were studied on Thermo Scientific Q Extractive series. Inverted fluorescence microscope (Nikon, Japan), carbon dioxide incubator (Thermo, USA), enzyme labeling instrument (Tecan, Switzerland). Cell lines: A549 (Kunming Cell Bank of Chinese Academy of Sciences), PC-3 (Kunming Cell Bank of Chinese Academy of Sciences), HepG2 (Kunming Cell Bank of Chinese Academy of Sciences), K562 (Kunming Cell Bank of Chinese Academy of Sciences).

Chemistry

The synthesis of intermediates 2

To the mixture of triphosgene (2.96 g, 10 mmol) in DCM (20 mL) was added dropwise to aniline derivatives (10 mmol) in DCM (20 mL), a large amount of white solids were produced. Then added

triethylamine (3 mL triethylamine dissolved in 7 mL DCM) slowly, followed a large amount of white smoke produced, the white solids were gradually dissolved and released a lot of heat. After the addition was completed, the solvent was removed on a rotary evaporator. The white solid intermediate **2** was obtained and the yield is 80%−90%.

The synthesis of intermediate 4

The solution NaOH (0.03 g, 7.453 mmol) and benzaldehydes were added to the mixture of 4-methylacetophenone (7.91 g, 74.53 mmol) and anhydrous EtOH (20 mL) stirring at room temperature. The white precipitation was produced after stirring about 5 h. If there was no white precipitation, the precipitation can be precipitated when hydrochloric acid was added to adjust the pH value to neutral at the end of the reaction. Reactions were monitored by TLC, and finally the solvent was evaporated under reduced pressure. The obtained white solid was recrystallized from EtOH to obtain purified intermediate **4** with a yield of 80−90%.

The synthesis of intermediate 5

Intermediate **4** (1.00 g, 4.50 mmol) was dissolved in EtOH (30 mL) in a 50 mL round bottom flask. Guanidine hydrochloride (4.50 mmol) and KOH (2.8 equiv.) were added to the solution. The mixture was refluxed for 10 h. After the reaction was completed (through TLC monitoring), the reaction mixture was cooled and poured into crushed ice, and the crude product was obtained through washing and drying. The purified intermediate **5** was obtained by recrystallizing from EtOH with a yield of 80−90%.

The synthesis of compounds HD-1-HD-17

Phenyl isocyanates intermediate **2** (26.79 mmol) was added into 4-phenyl-6-(*p*-methylphenyl)pyrimidinly-2-amine intermediate **5** (3.83 mmol) and the reaction was performed at 100 ℃ and produced white solids rapidly. After the reaction was completed (about 40 min through TLC monitoring), the white solid was recrystallized with CH_2Cl_2 to obtain a pure product.

1-(4-Phenyl-6-(*p*-tolyl)pyrimidin-2-yl)-3-(*p*-tolyl)urea (HD-1)

White solid, yield 65%, mp 176−178 ℃; ^{1}H NMR (500 MHz, DMSO-d_6) δ 11.62 (s, 1H), 10.12 (s, 1H), 8.28 – 8.25 (m, 2H), 8.19 (d, *J* = 8.2 Hz, 2H), 8.14 (s, 1H), 7.59 (d, *J* = 3.3 Hz, 2H), 7.44 (d, *J* = 8.4 Hz, 2H), 7.39 (d, *J* = 8.1 Hz, 2H), 7.29 – 7.26 (m, 1H), 7.15 (d, *J* = 8.3 Hz, 2H), 7.03 (d, *J* = 8.3 Hz, 1H), 2.39 (s, 3H), 2.24 (s, 3H). ^{13}C NMR (126 MHz, DMSO-d_6) δ 165.4, 165.3, 158.8, 153.1, 152.1, 142.2, 136.7, 136.6, 133.9, 132.5, 132.0, 130.2, 130.0, 129.7, 129.5, 127.9, 127.9, 119.6, 118.7, 106.8, 21.6, 20.9. HRMS (AP-ESI) *m/z* calcd for $C_{25}H_{21}ON_4$ $[M-H]^+$ 393.17099.19245, found 393.17175.

1-(4-Phenyl-6-(*p*-tolyl)pyrimidin-2-yl)-3-(*m*-tolyl)urea (HD-2)

White solid, yield 67%, mp 178−179 ℃; ^{1}H NMR (500 MHz, DMSO-d_6) δ 11.69 (s, 1H), 10.15 (s, 1H), 8.30 – 8.26 (m, 2H), 8.20 (d, *J* = 8.3 Hz, 2H), 8.15 (s, 1H), 7.59 (dd, *J* = 6.3, 2.7 Hz, 3H), 7.41 – 7.36 (m, 4H), 7.22 (t, *J* = 7.7 Hz, 1H), 6.86 (d, *J* = 7.5 Hz, 1H), 2.39 (s, 3H), 2.29 (s, 3H). ^{13}C NMR (126 MHz,

DMSO-d_6) δ 165.3, 158.8, 152.1, 142.2, 139.1, 138.8, 136.7, 133.8, 132.0, 130.1, 129.5, 128.0, 127.9, 124.2, 120.1, 116.6, 106.8, 21.8, 21.6. HRMS (AP-ESI) *m/z* calcd for $C_{25}H_{21}ON_4$ $[M-H]^+$ 393.17099.19245, found 393.17230.

1-(2-Chlorophenyl)-3-(4-phenyl-6-(*p*-tolyl)pyrimidin-2-yl)urea (HD-3)

White solid, yield 69%, mp 178−179 ℃; ^{1}H NMR (500 MHz, DMSO-d_6) δ 11.74 (s, 1H), 10.24 (s, 1H), 8.26 (s, 2H), 8.21 – 8.12 (m, 3H), 7.57 (d, *J* = 8.5 Hz, 5H), 7.40 (d, *J* = 7.6 Hz, 4H), 2.38 (s, 3H). ^{13}C NMR (126 MHz, DMSO-d_6) δ 165.5, 165.4, 158.7, 152.2, 142.2, 138.1, 136.6, 133.7, 132.0, 130.2, 129.6, 129.5, 127.9, 127.9, 127.2, 121.2, 106.96, 21.6. HRMS (AP-ESI) *m/z* calcd for $C_{24}H_{20}ClN_4O$ $[M+H]^+$ 415.13202, found 415.13126.

1-(3-Chlorophenyl)-3-(4-phenyl-6-(*p*-tolyl)pyrimidin-2-yl)urea (HD-4)

White solid, yield 66%, mp 176−177 ℃; ^{1}H NMR (500 MHz, DMSO-d_6) δ 11.82 (s, 1H), 10.28 (s, 1H), 8.26 (s, 2H), 8.20 – 8.12 (m, 3H), 7.79 (s, 1H), 7.58 (s, 3H), 7.44 – 7.33 (m, 4H), 7.10 (s, 1H), 2.38 (s, 1H). ^{13}C NMR (126 MHz, DMSO-d_6) δ 165.5, 165.4, 158.6, 152.2, 142.2, 140.7, 136.7, 132.0, 131.3, 130.2, 129.6, 128.0, 123.2, 119.1, 117.89, 107.1, 21.6. HRMS (AP-ESI) *m/z* calcd for $C_{24}H_{20}ClN_4O$ $[M+H]^+$ 415.13202, found 415.13144.

1-Benzyl-3-(4-phenyl-6-(*p*-tolyl)pyrimidin-2-yl)urea (HD-5)

White solid, yield 66%, mp 176−177 ℃; ^{1}H NMR (500 MHz, DMSO-d_6) δ 9.87 (s, 1H), 9.57 (s, 1H), 8.10 – 8.07 (m, 2H), 8.05 (s, 1H), 8.01 (d, *J* = 8.2 Hz, 2H), 7.53 – 7.48 (m, 1H), 7.44 (d, *J* = 7.9 Hz, 2H), 7.42 (dd, *J* = 3.9, 1.6 Hz, 1H), 7.39 (d, *J* = 6.7 Hz, 2H), 7.37 – 7.35 (m, 1H), 7.31 (dt, *J* = 9.5, 4.1 Hz, 1H), 7.25 (d, *J* = 8.2 Hz, 2H), 4.47 (d, *J* = 5.2 Hz, 2H), 2.34 (s, 3H). ^{13}C NMR (126 MHz, DMSO-d_6) δ 165.2, 165.1, 159.1, 154.5, 141.9, 139.5, 136.5, 133.7, 131.8, 130.0, 129.4, 129.2, 128.5, 127.9, 127.7, 106.10, 44.1, 21.6. HRMS (AP-ESI) *m/z* calcd for $C_{25}H_{23}N_4O$ $[M+H]^+$ 395.18664, found 395.18615.

1-(Naphthalen-1-yl)-3-(4-phenyl-6-(*p*-tolyl)pyrimidin-2-yl)urea (HD-6)

White solid, yield 80%, mp 182−183 ℃; ^{1}H NMR (500 MHz, DMSO-d_6) δ 11.87 (s, 1H), 10.38 (s, 1H), 8.29 – 8.26 (m, 2H), 8.21 (d, *J* = 8.2 Hz, 2H), 8.18 (s, 1H), 8.14 – 8.11 (m, 1H), 8.01 (d, *J* = 8.5 Hz, 1H), 7.97 (d, *J* = 8.2 Hz, 1H), 7.74 (d, *J* = 8.2 Hz, 1H), 7.60 (d, *J* = 7.2 Hz, 1H), 7.57 (d, *J* = 2.0 Hz, 1H), 7.56 – 7.51 (m, 3H), 7.36 (d, *J* = 8.2 Hz, 2H), 7.19 (s, 1H), 2.41 (s, 3H). ^{13}C NMR (126 MHz, DMSO-d_6) δ 165.8, 165.8, 159.1, 152.7, 142.1, 136.8, 134.2, 134.0, 133.8, 131.8, 130.1, 129.5, 129.0, 128.2, 128.1, 126.6, 126.4, 124.5, 122.0, 119.4, 107.6, 21.6. HRMS (AP-ESI) *m/z* calcd for $C_{28}H_{23}N_4O$ $[M+H]^+$ 431.18664, found 431.18701.

1-(4-Chlorophenyl)-3-(4-phenyl-6-(*p*-tolyl)pyrimidin-2-yl)urea (HD-7)

White solid, yield 68%, mp 179−180 ℃; ^{1}H NMR (500 MHz, DMSO-d_6) δ 11.79 (s, 1H), 10.30 (s, 1H), 8.31 (s, 2H), 8.26 – 8.18 (m, 3H), 7.63 (s, 5H), 7.44 (d, *J* = 7.1 Hz, 4H), 2.43 (s, 3H). ^{13}C NMR (126 MHz, DMSO-d_6) δ 165.4, 165.4, 158.7, 152.1, 142.2, 138.1, 136.6, 133.8, 132.0, 130.2, 129.6, 129.5,

127.9, 127.9, 127.1, 121.1, 107.0, 21.6. HRMS (AP-ESI) *m/z* calcd for $C_{24}H_{19}ClN_4O$ $[M+H]^+$ 415.13202, found 415.13156.

1-(4-Fluorophenyl)-3-(4-phenyl-6-(*p*-tolyl)pyrimidin-2-yl)urea (HD-8)

White solid, yield 71%, mp 178−179 ℃; ^{1}H NMR (500 MHz, DMSO-d_6) δ 11.67 (s, 1H), 10.19 (s, 1H), 8.27 (s, 2H), 8.21 – 8.12 (m, 3H), 7.58 (s, 5H), 7.39 (d, *J* = 7.0 Hz, 2H), 7.19 (s, 2H), 2.38 (s, 3H). ^{13}C NMR (126 MHz, DMSO-d_6) δ 165.4, 158.8, 152.3, 142.2, 136.7, 133.8, 132.0, 130.2, 129.6, 127.9, 121.4, 116.3, 116.1, 106.9, 21.6. HRMS (AP-ESI) *m/z* calcd for $C_{24}H_{20}FN_4O$ $[M+H]^+$ 399.16157, found 399.16107.

1-(4-(4-Methoxyphenyl)-6-(*p*-tolyl)pyrimidin-2-yl)-3-(*m*-tolyl)urea (HD-9)

White solid, yield 74%, mp 179−180 ℃; ^{1}H NMR (500 MHz, DMSO-d_6) δ 11.79 (s, 1H), 10.15 (s, 1H), 8.32 – 8.30 (m, 2H), 8.22 (d, *J* = 8.2 Hz, 2H), 8.13 (s, 1H), 7.45 – 7.41 (m, 3H), 7.29 – 7.24 (m, 1H), 7.18 – 7.15 (m, 2H), 6.91 (d, *J* = 7.5 Hz, 1H), 3.88 (s, 3H), 2.43 (s, 3H), 2.33 (s, 3H). ^{13}C NMR (126 MHz, DMSO-d_6) δ 164.4, 161.9, 158.0, 151.5, 138.2, 133.3, 129.5, 129.0, 128.9, 127.2, 123.5, 119.4, 116.0, 114.2, 105.3, 55.4, 21.2, 20.9. HRMS (AP-ESI) *m/z* calcd for $C_{26}H_{25}N_4O_2$ $[M+H]^+$ 425.19720, found 425.19666.

1-(4-(4-Methoxyphenyl)-6-(*p*-tolyl)pyrimidin-2-yl)-3-(*p*-tolyl)urea (HD-10)

White solid, yield 76%, mp 178−179 ℃; ^{1}H NMR (500 MHz, DMSO-d_6) δ 11.78 (s, 1H), 10.15 (s, 1H), 8.31 (d, *J* = 8.9 Hz, 2H), 8.22 (d, *J* = 8.2 Hz, 2H), 8.13 (s, 1H), 7.43 (dd, *J* = 11.3, 7.2 Hz, 4H), 7.29 – 7.24 (m, 1H), 7.16 (d, *J* = 8.9 Hz, 2H), 6.91 (d, *J* = 7.6 Hz, 1H), 3.88 (s, 3H), 2.43 (s, 3H), 2.33 (s, 3H). ^{13}C NMR (126 MHz, DMSO-d_6) δ 164.9, 162.6, 158.7, 152.2, 142.1, 139.1, 138.9, 134.0, 130.1, 129.7, 129.6, 128.9, 127.8, 124.2, 120.1, 116.6, 114.9, 105.9, 56.0, 21.8, 21.6. HRMS (AP-ESI) *m/z* calcd for $C_{26}H_{23}N_4O_2$ $[M-H]^+$ 423.18155, found 423.18167.

1-(2-Chlorophenyl)-3-(4-(4-methoxyphenyl)-6-(*p*-tolyl)pyrimidin-2-yl)urea (HD-11)

White solid, yield 78%, mp 179−180 ℃; ^{1}H NMR (500 MHz, DMSO-d_6) δ 11.80 (s, 1H), 10.34 (s, 1H), 8.28 (d, *J* = 8.9 Hz, 2H), 8.18 (d, *J* = 8.2 Hz, 2H), 8.08 (s, 1H), 7.83 (s, 1H), 7.38 (t, *J* = 7.8 Hz, 3H), 7.34 (d, *J* = 8.9 Hz, 1H), 7.14– 7.09 (m, 3H), 3.84 (s, 3H), 2.45 (s, 3H). ^{13}C NMR (126 MHz, DMSO-d_6) δ 165.1, 162.6, 158.5, 152.2, 142.0, 140.7, 133.9, 131.3, 130.1, 129.7, 128.8, 127.9, 123.1, 119.1, 117.9, 114.9, 106.2, 56.0, 21.6. HRMS (AP-ESI) *m/z* calcd for $C_{26}H_{23}N_4O_2$ $[M-H]^+$ 445.14258, found 445.14230.

1-(3-Chlorophenyl)-3-(4-(4-methoxyphenyl)-6-(*p*-tolyl)pyrimidin-2-yl)urea (HD-12)

White solid, yield 79%, mp 178−179 ℃; ^{1}H NMR (500 MHz, DMSO-d_6) δ 11.89 (s, 1H), 10.24 (s, 1H), 8.25 (d, *J* = 8.9 Hz, 2H), 8.16 (d, *J* = 8.2 Hz, 2H), 8.08 (s, 1H), 7.82 (s, 1H), 7.37 (t, *J* = 7.8 Hz, 3H), 7.32 (d, *J* = 8.9 Hz, 1H), 7.12 – 7.08 (m, 3H), 3.83 (s, 3H), 2.38 (s, 3H). ^{13}C NMR (126 MHz, DMSO-d_6) δ 165.1, 162.6, 158.5, 152.2, 142.1, 140.7, 133.9, 131.3, 130.1, 129.7, 128.8, 127.8, 123.1, 119.1, 117.9,

114.9, 106.2, 56.0, 21.6. HRMS (AP-ESI) *m/z* calcd for $C_{25}H_{22}ClN_4O_2$ $[M+H]^+$ 445.14258, found 445.14194.

1-(4-Chlorophenyl)-3-(4-(4-methoxyphenyl)-6-(*p*-tolyl)pyrimidin-2-yl)urea (HD-13)

White solid, yield 78%, mp 178−179 ℃; ^{1}H NMR (500 MHz, DMSO-d_6) δ 11.89 (s, 1H), 10.24 (s, 1H), 8.26 (d, *J* = 8.9 Hz, 2H), 8.17 (d, *J* = 8.2 Hz, 2H), 8.09 (s, 1H), 7.82 (s, 1H), 7.37 (t, *J* = 8.2 Hz, 2H), 7.33 (d, *J* = 8.5 Hz, 1H), 7.10 (dd, *J* = 9.6, 4.9 Hz, 3H), 3.83 (s, 3H), 2.38 (s, 3H). ^{13}C NMR (126 MHz, DMSO-d_6) δ 165.1, 162.6, 158.5, 152.2, 142.0, 140.7, 133.9, 131.3, 130.1, 129.7, 128.8, 127.9, 123.1, 119.1, 117.9, 114.9, 106.2, 56.0, 21.6. HRMS (AP-ESI) *m/z* calcd for $C_{25}H_{22}ClN_4O_2$ $[M+H]^+$ 445.14258, found 445.14230.

1-(3-Fluorophenyl)-3-(4-(4-methoxyphenyl)-6-(*p*-tolyl)pyrimidin-2-yl)urea (HD-14)

White solid, yield 76%, mp 177−178 ℃; ^{1}H NMR (500 MHz, DMSO-d_6) δ 11.73 (s, 1H), 10.15 (s, 1H), 8.70 (s, 2H), 8.26 (d, *J* = 8.0 Hz, 1H), 8.17 (d, *J* = 7.4 Hz, 1H), 8.09 (s, 1H), 7.56 (s, 1H), 7.40 (s, 4H), 7.19 (s, 1H), 7.12 (d, *J* = 8.1 Hz, 1H), 7.07 (s, 1Hv), 3.83 (s, 3H), 2.38 (s, 3H). ^{13}C NMR (126 MHz, DMSO-d_6) δ 165.1, 162.6, 158.6, 152.2, 142.0, 140.7, 134.0, 131.3, 130.1, 129.7, 128.9, 127.9, 123.1, 119.1, 117.9, 114.9, 106.2, 56.0, 21.6. HRMS (AP-ESI) *m/z* calcd for $C_{25}H_{22}FN_4O_2$ $[M+H]^+$ 429.17213, found 429.17188.

1-(4-(4-Methoxyphenyl)-6-(*p*-tolyl)pyrimidin-2-yl)-3-(3-(trifluoromethyl)phenyl)urea (HD-15)

White solid, yield 75%, mp 179−180 ℃; ^{1}H NMR (500 MHz, DMSO-d_6) δ 11.81 (s, 1H), 10.21 (s, 1H), 8.27 (s, 1H), 8.17 (d, *J* = 8.2 Hz, 2H), 8.10 (s, 1H), 7.58 (d, *J* = 8.9 Hz, 2H), 7.45 – 7.41 (m, 2H), 7.40 (d, *J* = 2.1 Hz, 2H), 7.28 (d, *J* = 8.9 Hz, 1H), 7.13 (d, *J* = 9.0 Hz, 2H), 3.84 (s, 3H), 2.39 (s, 3H). ^{13}C NMR (126 MHz, DMSO-d_6) δ 165.0, 164.8, 164.4, 161.7, 142.4, 141.9, 140.6, 135.2, 130.2, 129.8, 129.7, 129.1, 127.4, 126.1, 114.4, 101.2, 55.8, 21.5, 21.4. HRMS (AP-ESI) *m/z* calcd for $C_{26}H_{20}F_3N_4O_2$ $[M+H]^+$ 477.15329, found 477.15152.

1-Benzyl-3-(4-(4-methoxyphenyl)-6-(*p*-tolyl)pyrimidin-2-yl)urea (HD-16)

White solid, yield 73%, mp 184−185 ℃; ^{1}H NMR (500 MHz, DMSO-d_6) δ 9.82 (s, 1H), 9.62 (s, 1H), 8.06 (d, *J* = 8.9 Hz, 2H), 7.98 (d, *J* = 8.6 Hz, 3H), 7.40 – 7.37 (m, 3H), 7.34 – 7.30 (m, 1H), 7.24 – 7.21 (m, 2H), 6.96 (d, *J* = 9.0 Hz, 2H), 4.46 (d, *J* = 5.2 Hz, 2H), 3.80 (s, 3H), 2.33 (s, 3H). ^{13}C NMR (126 MHz, DMSO-d_6) δ 164.7, 164.6, 162.3, 159.0, 154.6, 141.8, 139.5, 133.8, 123.0, 129.4, 129.2, 128.7, 128.7, 128.5, 127.9, 127.6, 127.5, 127.1, 114.7, 105.2, 55.9, 44.1, 21.5. HRMS (AP-ESI) *m/z* calcd for $C_{26}H_{25}N_4O_2$ $[M+H]^+$ 425.19720, found 429.19661.

1-(4-(4-Methoxyphenyl)-6-(*p*-tolyl)pyrimidin-2-yl)-3-(naphthalen-1-yl)urea (HD-17)

White solid, yield 78%, mp 184−185 ℃; ^{1}H NMR (500 MHz, DMSO-d_6) δ 11.85 (s, 1H), 10.27 (s, 1H), 8.23 (d, *J* = 8.9 Hz, 2H), 8.13 (d, *J* = 8.2 Hz, 2H), 8.06 (dd, *J* = 5.9, 5.5 Hz, 2H), 7.94 (dd, *J* = 19.1, 8.3 Hz, 2H), 7.70 (d, *J* = 8.2 Hz, 1H), 7.50 (td, *J* = 7.5, 5.3 Hz, 2H), 7.29 (d, *J* = 8.1 Hz, 2H), 7.21 – 7.16 (m,

1H), 7.03 (d, *J* = 8.9 Hz, 2H), 3.80 (s, 3H), 2.35 (s,3H). ^{13}C NMR (126 MHz, DMSO-d_6) δ 165.4, 165.3, 162.5, 159.0, 152.8, 141.8, 134.2, 134.0, 134.0, 130.0, 129.9, 129.0, 128.9, 128.0, 126.7, 126.7, 126.5, 126.4, 124.5, 122.0, 119.6, 114.8, 106.6, 56.0, 21.6. HRMS (AP-ESI) *m/z* calcd for $C_{29}H_{25}N_4O_2$ $[M+H]^+$ 461.19720, found 461.19678.

Biological activity

MTT assay

The *in vitro* inhibitory activity of the target compounds against A549, PC-3, K562 and HepG2 tumor cell lines were tested by MTT method. The logarithmic cells were cultured in a 96-well plate and pre-cultured for 24 h before adding the test compound. Then different concentrations of 20 μL compound solution were added to the 96-well plate. After the cells were cultured at 37 ℃ and 5% carbon dioxide for 48 h, 20 μL tetramethylazolium salt solution with a concentration of 5 μg/mL was added and reacted in the same environment for 4 h, and the absorbance was measured at 490 nm by microplate reader (Tecan, Infinite M200 Pro).

DAPI staining experiment

PC-3 cells were inoculated in a 6-well plate with a density of 5×10^4 cells per well and pre-cultured for 24 h, the cells were treated with different concentrations of compound **HD-6**, while the negative well was the same amount of DMSO. After 24 h of culturing in the incubator, the cells were fixed with 4% paraformaldehyde for 10 min, and stained with DAPI staining solution for 10 min, finally sealed with water-soluble sealing agent and the results were imaged by an inverted fluorescence microscope.

Flow cytometry apoptosis experiment

PC-3 cells were inoculated in a 6-well plate with a density of 5×10^4 cells per well and pre-cultured for 24 h, the cells were treated with different concentrations of compound **HD-6**, while the negative well was the same amount of DMSO. The cells were collected after being cultured in the incubator for 48 h. After adding 100 μL binding buffer per tube, PC-3 cells were stained with Annexin V-FITC and propidium iodide for 20 min. Finally, the surviving, early apoptotic, late apoptotic and necrotic cells were classified by flow cytometry.

ROS level detection experiment

PC-3 cells were inoculated in a 6-well plate with a density of 5×10^4 cells per well and pre-cultured for 24 h, the cells were treated with different concentrations of compound **HD-6**, while the negative well was the same amount of DMSO. The cells were collected after being cultured in the incubator for 24 h. Added fluorescent probe DCFH-DA and cultured in the incubator for 20 min. Finally, the level of reactive oxygen species in PC-3 cells was detected by flow cytometry.

Cell Cycle Analysis

PC-3 cells were inoculated in a 6-well plate with a density of 6×10^4 cells per well and pre-cultured for 24

h, the cells were treated with different concentrations of compound **HD-6**, while the negative well was the same amount of DMSO. After 24 h of culturing in the incubator, the cells were collected and incubated in 37 ℃ water bath for 30 min after adding 100 μL RNase. After incubation, PC-3 cells were stained with 400 μL propidium iodide in refrigerator at 4 ℃. Flow cytometry was used to detect the cell cycle.

Western blotting

PC-3 cells were managed with compound **HD-6** at 12 μM for 36 h and sorafenib at 12 μM as the control. After treatment, these cells were collected and segregated via adopting RIPA lysis buffer with the correlative protease inhibitors. The BCA Protein Assay Kit was carried out for determination of total protein concentration. Thirty micrograms of protein samples were segregated through utilizing 10% SDS-PAGE, and next transferred onto PVDF membranes and blocked at room temperature for 150 min. The befitting primary antibodies include EGFR, phosphorylated (p)-EGFR and β-Actin were sealed in Antibody Dilution Buffer, and cocultivated with the PVDF membrane at 4 ℃ overnight. After this, the second antibody was replenished and cofostered with the above membrane for additional 1 h at room temperature. An enhanced chemiluminescent kit was then used to conduct chemiluminescent detection.

ACKNOWLEDGEMENTS

This work was supported by the National Natural Science Foundation of China (22007022, 21867004), Guizhou Provincial Natural Science Foundation (ZZK[2021]) and Top Science and Technology Talent Program of Guizhou Education Department ([2022]075).

SUPPORTING INFORMATION

Additional supporting information including ^{1}H, ^{13}C NMR and HRMS spectra of compounds **HD-1**-**HD-17** may be found online in the Supporting Information section at the end of the article.

REFERENCES

1. E. Abdelghani, S. A. Said, M. G. Assy, and A. M. Abdel Hamid, *Arab. J. Chem.*, 2017, **10**, S2926.
2. N. E. A. Abd El-Sattar, E. H. K. Badawy, and M. S. A. Abdel-Mottaleb, *J. Chem.*, 2018, 8795061.
3. N. B. Kayathi, D. V. Sowmya, P. Adivireddy, and P. Venkatapuram, *J. Heterocycl. Chem.*, 2018, **55**, 1024.
4. K. Irena and A. Y. Petar, *Curr. Org. Chem.*, 2017, **21**, 2096.
5. N. Polish, M. Nesterkina, N. Marintsova, A. Karkhut, I. Kravchenko, V. Novikov, and A. Khairulin, *Acta Chim. Slov.*, 2020, **67**, 934.
6. R. Soto-Acosta, E. Jung, L Qiu, D. J. Wilson, R. J. Geraghty, and L. Q. Chen, *Molecules*, 2021, **26**, 3779.

7. M. K. Pradip, *Curr. Org. Chem.*, 2020, **24**, 1055.
8. P. Yadav and K. Shah, *Chem. Biol. Drug Des.*, 2020, **97**, 633.
9. M. Hou, Y. Y. Zou, S. L. Fan, X. Q. Li, L. H. Shao, Z. R. Li, D. P. Chen, Z. C. Wang, and G. P. Ouyang, *J. Heterocycl. Chem.*, 2022, **59**, 1025.
10. X. Gao, L. Cen, F. Li, R. Wen, H. Yan, H. Yao, and S. Zhu, *Biochem. Biophys. Res. Commun.*, 2018, **505**, 761.
11. F. Safaria, M. Bayatb, S. Nasrib, and S. Karamib, *Bioorg. Med. Chem. Lett.*, 2020, **30**, 10.
12. R. Surendrakumar, A. Idhayadhulla, S. Alarifi, N. A. Ahamed, and C. S. Kumar, *Biomed. Res. Int.*, 2020, 8872479.
13. B. Q. Gong, F. Hong, C. Kohm, S. Jenkins, J. Tulinsky, R. Bhatt, P. D. Vries, J. W. Singer, and P. Klein, *Bioorg. Med. Chem. Lett.*, 2004, **14**, 2303.
14. L. Pan, Z. Liu, Y. W. Chen, Y. H. Li, and Z. M. Li, *Chem. J. Chinese Univ.*, 2013, **34**, 6.
15. S. Hawser, S. Lociuro, and K. Islam, *Biochem. Pharmacol.*, 2006, **71**, 941.
16. J. L. Bernier, J. P. Henichart, V. Warin, and F. Baert, *J. Pharm. Sci.*, 1980, **69**, 1343.
17. D. Hocková, A. Holý, M. Masojídková, G. Andrei, R. Snoeck, E. De Clercq, and J. Balzarini, *J. Med. Chem.*, 2003, **46**, 5064.
18. W. K. Guo, Y. J. Xing, Q. S. Zhang, J. Q. Xie, D. X. Huang, H. J. Gu, P. He, M. Zhou, S. F. Xu, X. F. Pang, M. Y. Liu, Z. F. Yi, and Y. H. Chen, *J. Med. Chem.*, 2020, **63**, 676.
19. L. Y. Liu, Z. C. Tang, C. Z. Wu, X. Y. Li, A. L. Huang, X. Lu, Q. D. You, and H. Xiang, *Bioorg. Med. Chem. Lett.*, 2018, **28**, 1138.
20. J. Zimmermann, G. Caravatti, H. Mett, T. Meyer, M. Müller, N. B. Lydon, and D. Fabbro, *Arch. Pharm.*, 1996, **329**, 371.
21. L. Garuti, M. Roberti, G. Bottegoni, and M. Ferraro, *Curr. Med. Chem.*, 2016, **23**, 1528.
22. B. M. Sahoo, B. K. Banik, P. Borah, and A. Jain, *Anticancer Agents Med. Chem.*, 2022, **22**, 215.
23. C. R. Reczek and N. S. Chandel, *Annu. Rev. Cancer Biol.*, 2017, **1**, 79.
24. H. Yang, R. M. Villani, H. Wang, M. J. Simpson, M. S. Roberts, M. Tang, and X. W. Liang, *J. Exp. Clin. Canc. Res.*, 2018, **37**, 266.
25. M. A. Shaha and H. A. Rogoff, *Semin. Oncol.*, 2021, **48**, 3.
26. C. J. Sherr and J. Bartek, *Annu. Rev. Cancer Biol.*, 2017, **1**, 41.